Letter to the Editor

Glyphosate Based-Herbicide Induced Nephrotoxicity through Oxidative Stress and the Imbalance of Osmotic Pressure in Mice*

Lei Qi[1,2,3], Jinfeng Zhu[1], Yanbo Qi[1], Hong Chao[1], Yu Cheng[1], Xiaolei Yang[1], Hongjie Li[1], Gang Li[1,2,#], and Jicheng Liu[2,3,#]

Glyphosate-based herbicides (GBHs) are used for weeding purposes in orchards and rubber plantations, as well as in the cultivation of tea mulberry and genetically modified crops. In recent years, GBH has become the most widely used organic phosphorus pesticide. Glyphosate and its metabolites can easily chelate metals, resulting in the formation of persistent residues that are frequently detected in natural environments. Recently, an increasing number of past studies have indicated that glyphosate exposure may be a risk factor for mental disease, liver, and tumorigenesis[1,2]. Therefore, the widespread use of GBHs poses potential public health risks.

Within agricultural populations in Sri Lanka, glyphosate application *via* spraying is associated with chronic kidney disease of unknown etiology[3]. Occupational exposure to glyphosate can induce kidney toxicity. In rodents, GBHs induce histopathological injury characterized by glomerular damage, degeneration of tubular epithelial cells, and inflammation and necrosis of renal tubules[4]. Furthermore, GBH exposure is associated with increased serum levels of biochemical markers of kidney function, including bilirubin, urea, and creatinine. Oxidative stress (OS) plays a key role in the mechanism of glyphosate-induced nephrotoxicity. Specifically, Glyphosate or GBHs induce reactive oxygen species (ROS) generation and promote malondialdehyde (MDA) production, while lowering the activity of antioxidant enzymes and substances in the kidney[5]. Nevertheless, the mechanism of xenobiotic toxicity is complex and a systematic investigation of the specific metabolic regulatory mechanism of GBH-induced nephrotoxicity has not yet been reported.

Environmental metabolomics has been widely used to investigate the effects of environmental toxins on aquatic organisms and mammals. Metabolomics has two advantages in investigating the interactions between xenobiotics and health. First, it allows for the screening of biomarkers *via* high-throughput and sensitive data analysis. Second, it allows the use of enriched biochemical pathways related to the identified metabolites to depict a network of toxic mechanisms. In the current study, metabolomics was used to illustrate the toxic effects of GBH exposure on the kidneys and the associated biological mechanisms.

In this study, male Kunming mice were exposed to different doses of a GBH (0, 50, 250, and 500 mg/kg per day) in the normal control (NC) group, low-dose GBH (LG) group, medium-dose GBH (MG) group and high-dose GBH (HG) group for 30 days, respectively. Alterations in renal pathological and functional parameters, oxidative stress, and metabolomics were assessed as described in Supplementary Methods (available in www.besjournal.com). The pathological changes and kidney function parameters were evaluated to assess the nephrotoxic effects of the GBH. As shown in Supplementary Figure S1 (available in www.besjournal.com), GBH administration resulted in no significant differences in body weight, kidney viscera

doi: 10.3967/bes2024.178

*This work was supported by the Fundamental Research Funds for the Department of Education in Heilongjiang Province (Grant No. 2020-KYYWF-0037 and No. 2019-KYYWF-1277); National Natural Science Foundation of China (No. 82103869); Project of Qiqihar Academy of Medical Sciences (Grant No. QMSI2019M-23, No. QMSI2019M-05 and No. 2024-ZDPY-003); Technology Plan Joint Guidance Project of Qiqihar (Grant No. LHYD-202007); Doctor Youth Fund of Qiqihar Academy of Medical Sciences (Grant No. QMSI2023B-13); and Technology Plan Joint Guidance Project of Qiqihar (Grant No. LSFGG-2024100).

1. School of Public Health, Qiqihar Medical University, Qiqihar 161006, Heilongjiang, China; 2. Qiqihar Academy of Medical Sciences, Qiqihar 161006, Heilongjiang, China; 3. Postdoctoral Research Station of Qiqihar Institute of Medical Science, Qiqihar 161006, Heilongjiang, China

coefficient, and uric acid (UA) level between mice in the NC, LG, MG, and HG groups. Mice in the HG group showed significantly higher creatinine (CRE), urea nitrogen (BUN) and β-N-acetylaminoglucosidase (NAG) levels than those in the NC group ($P < 0.05$). Moreover, when compared with the NC group, the renal epithelial cells of mice in the MG group showed slight edema, whereas those of mice in the HG group exhibited renal tubular epithelial water degeneration, swelling, and abundant protein deposition in the renal tubules (Figure 1). These observations indicated a correlation between GBH treatment and nephrotoxicity.

Oxidative stress, induced by ROS overproduction, is a major pathogenic factor in GBH-induced nephrotoxicity. Generally, ROS are generated *via* an endogenous metabolism and are beneficial for cellular signal transduction and internal balance. However, excessive ROS generation disrupts the oxidative-antioxidant system and damages DNA, proteins, and lipids. As shown in Supplementary Figure S2 (available in www.besjournal.com), the MG and HG groups showed lower glutathione (GSH), total antioxidant capacity (T-AOC), catalase (CAT), and superoxide dismutase (SOD) levels than the NC group ($P < 0.05$), whereas an increase in the level of MDA ($P < 0.05$), one of the final product of lipid peroxidation, was observed in the HG group. These observations indicate that the oxidant-antioxidant balance is disrupted in the kidneys. However, the mechanism underlying the interaction between renal pathogenesis and dysfunction owing to OS remains unclear. Therefore, in order to provide clarification on this matter, we performed renal metabolomics to compare differences in metabolite composition and metabolic pathways between the NC and HG groups.

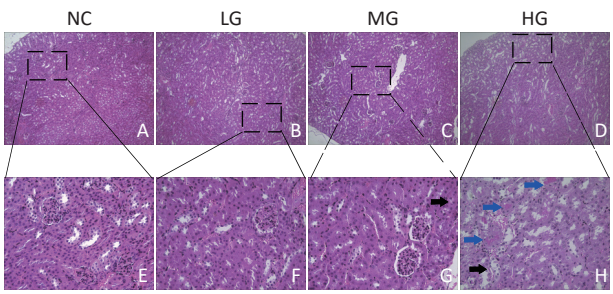

Figure 1. Effect of GBH exposure on histopathology in kidneys of male mice. A, B, C, and D, 100×; E, F, G, and H, 400×. Black arrow: water degeneration; blue arrow: protein deposition in renal tubules. NC, normal control group; LG, low dose group; MG, middle dose group; HG, high dose group.

As shown in Figures 2A and B, a distinct separation was observed between the HG and NC groups in the positive and negative ion modes. The permutation test results suggested that the OPLS-DA model used in the present study was stable (Supplementary Figure S3, available in www.besjournal.com). Furthermore, 44 and 22 significantly altered metabolites (SCMs) were identified according to $P < 0.05$, and the value of the variable importance in the projection (VIP) was > 1 in the positive and negative ion modes (Supplementary Figure S4, Supplementary Tables S1 and S2, available in www.besjournal.com). To clarify the effects of the GBH on metabolism, all SCMs were mapped to the Kyoto Encyclopedia of Genes and Genomes databases (KEGG). Ten and fourteen KEGG pathways were enriched in the positive and negative ion modes, respectively (Figure 2C and D, Supplementary Tables S3 and S4, available in www.besjournal.com). VB6 plays a critical role in the synthesis of GSH by activating nuclear factor E2-related factor 2 (Nrf2) signaling[6]. In the present study, the GBH decreased the levels of pyridoxal and pyridoxamine, perturbed the VB6 metabolic pathway, and inhibited GSH generation, suggesting that GBH induces kidney injury by blocking the antioxidant capacity of GSH *via* the VB6 metabolic pathway. A previous study showed that L-arginine improves antioxidant capacity by promoting the expression of antioxidant enzymes and decreasing MDA levels[7]. Moreover, L-arginine reduces renal OS caused by excessive NO generation by activating the Nrf2 signaling pathway[8]. In this study, we observed that GBH administration reduced the levels of L-arginine and argininosuccinic acid and disrupted arginine and proline metabolic pathways. These observations suggest that arginine metabolism disorder is a critical factor in GBH-induced renal OS.

Nitric oxide, which is synthesized from L-arginine by nitric oxide synthase (NOS), plays an important role in regulating renal blood flow and osmotic pressure[9]. The decrease in L-arginine levels observed in this study suggests that GBH may disturb renal osmotic pressure. The evidence shows that in the kidneys, choline and its metabolite, betaine aldehyde, are two osmotic protective agents for renal cells because they facilitate the reabsorption of water from the renal tubules[10]. In this study, GBH exposure reduced the levels of choline and betaine aldehyde, further disturbing the glycine, serine, and threonine metabolic pathways and confirming the toxic effects of GBH on renal osmotic pressure. Moreover, significant correlations were observed

between the levels of metabolites involved in osmotic pressure dysfunction and renal function indicators, the levels of metabolites involved in antioxidant capacity and OS indicators, and the levels of metabolites involved in antioxidant capacity and renal function, OS, and renal function indicators (Supplementary Figure S5, available in www.besjournal.com). These findings demonstrate that the GBH induces pathological and functional renal damage by triggering OS and osmotic pressure dysfunction.

Glucose utilization for energy production in renal cells is necessary for maintaining normal kidney function. In general, glucose is metabolized to pyruvate by a series of enzymes. Thereafter, pyruvate is utilized in the mitochondria to generate energy *via* the tricarboxylic acid cycle and oxidative phosphorylation. Thiamine is a vitamin that acts as a cofactor for many enzymes involved in aerobic glucose oxidation such as pyruvate dehydrogenase and alpha-ketoglutarate dehydrogenases. In this study, the GBH perturbed glycolysis, gluconeogenesis, and thiamine metabolism in the kidneys, indicating that GBH administration induced renal glucose utilization and potential energy metabolism disorders.

In conclusion, our results revealed that exposure to GBH induces renal tubular epithelial injury and dysfunction by inducing OS and disrupting metabolite balance in the kidneys. Notably, GBH administration disrupted VB6 and L-arginine metabolism, energy metabolism, and choline metabolism, thus promoting renal OS and osmotic pressure imbalance, resulting in pathological renal injury and dysfunction (Figure 3). However, this study has some limitations. First, the GBH dose administered to the mice in the HG group exceeded the actual exposure levels within the population. Secondly, GBH contains other auxiliary components, and we did not investigate whether the nephrotoxicity observed in this study was induced by glyphosate alone or by the combined effect of glyphosate and auxiliary components. Therefore, further studies focusing on actual exposure conditions and the effects of auxiliary components

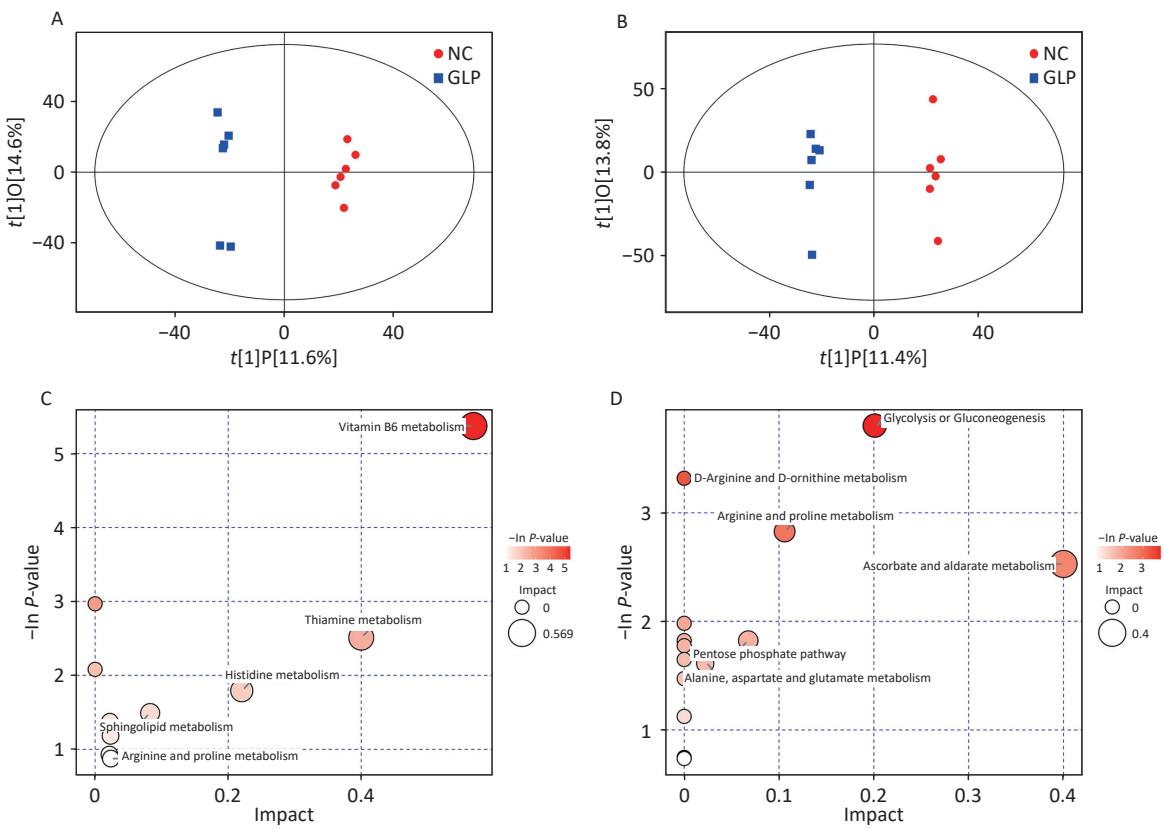

Figure 2. Effects of the GBH on global metabolomics profiles and metabolic pathways in the kidney. (A) and (B), OPLS-DA score plots from the positive and negative ion modes, respectively. (C) and (D), bubble chart of metabolic pathway analysis between HG and NC groups in the positive and negative ion modes, respectively. Each bubble in the bubble chart represents a metabolic pathway.

are necessary to identify new aspects of glyphosate- and GBH-induced nephrotoxicity health risks.

Conflicts of Interest The authors declare no conflict of interest.

Author Contributions Lei Qi: Investigation, methodology, data curation, formal analysis, funding acquisition, and writing- original draft. Jinfeng Zhu: Investigation, methodology, and data curation. Yanbo Qi: Methodology and resources. Hong Chao: Resources and funding acquisition. Yu Cheng: Methodology, visualization and software. Xiaolei Yang: Methodology and funding acquisition. Hongjie Li: Investigation, and methodology. Gang Li: Conceptualization, supervision, writing-review &

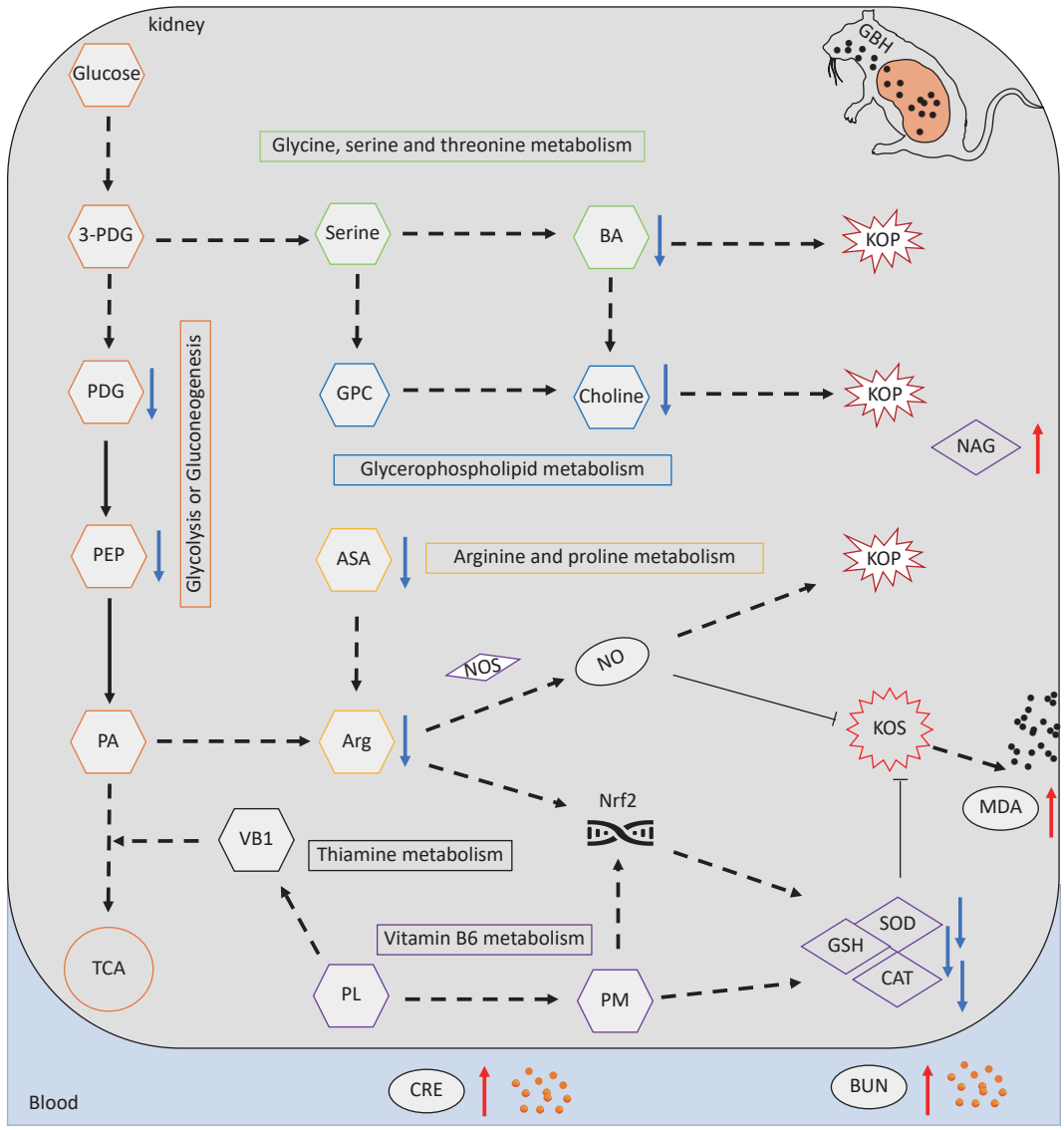

Figure 3. Mechanism of GBH-induced nephrotoxicity. Rectangle, metabolism pathways; hexagon, metabolites; diamond, enzymes. When compared with the control group, the red arrow depicts upregulation and blue arrow depicts downregulation. Black solid line arrow, direct reaction; dotted line arrow, multi-step reaction. PL, pyridoxal; PM, pyridoxamine; GA, D-Glucuronic acid; PDG, phospho-D-glyceric acid; PEPA, phosphoenolpyruvic acid; PA, Pyruvate; TCA, tricarboxylic acid cycle; Arg, L-arginine; ASA, argininosuccinic acid; BA, betaine aldehyde; NOS, nitric oxide synthase; Nrf2, nuclear factor erythroid2-related factor 2; KOS, kidney oxidative stress; KOP, kidney osmotic pressure; GSH, glutathione; CAT, catalase; SOD, superoxide dismutase; CRE, creatinine; BUN, urea nitrogen; NAG, β-N-acetylaminoglucosidase; MDA, malondialdehyde.

editing, and funding acquisition. Jicheng Liu: Supervision, and writing-review & editing.

#Correspondence should be addressed to Gang Li, PhD, Tel: 86-452-2663410; E-mail: ligang_xl@sina.com; Jicheng Liu, PhD, Tel: 86-452-2663290, qyybliu@163.com

Biographical note of the first author: Lei Qi, female, born in 1990, PHD, majoring in nutrition and food hygiene.

Received: June 19, 2024;

Accepted: September 19, 2024

REFERENCES

1. Martins-Gomes C, Silva TL, Andreani T, et al. Glyphosate vs. glyphosate-based herbicides exposure: a review on their toxicity. J Xenobiot, 2022; 12, 21−40.
2. Eskenazi B, Gunier RB, Rauch S, et al. Association of lifetime exposure to glyphosate and aminomethylphosphonic acid (AMPA) with liver inflammation and metabolic syndrome at young adulthood: findings from the CHAMACOS study. Environ Health Perspect, 2023; 131, 037001.
3. Ulrich JC, Hoffman K, Gunasekara TDKSC, et al. Glyphosate and fluoride in high-hardness drinking water are positively associated with chronic kidney disease of unknown etiology (CKDu) in Sri Lanka. Environ Sci Technol Lett, 2023; 10, 916−23.
4. Djaber N, Ounaceur LS, Moubine BN, et al. Roundup-induced biochemical and histopathological changes in the liver and kidney of rats: the ameliorative effects of Linum usitatissimum oil. Acta Biochim Pol, 2020; 67, 53−64.
5. Hassan MA, Hozien ST, Abdel Wahab MM, et al. Ameliorative effect of selenium yeast supplementation on the physio-pathological impacts ofchronic exposure to glyphosate and or malathion in *Oreochromis niloticus*. BMC Vet Res, 2022; 18, 159.
6. Mizutani T, Yamawaki Y, Okano Y, et al. Pyridoxine (VB_6) restores the down-regulation of serine palmitoyltransferase mRNA expression in keratinocytes cultured in highly oxidative conditions through enhancement of the intracellular antioxidant system. Exp Dermatol, 2019; 28 Suppl 1, 43-9.
7. Liang M C, Wang Z X, Li H, et al. l-Arginine induces antioxidant response to prevent oxidative stress via stimulation of glutathione synthesis and activation of Nrf2 pathway. Food Chem Toxicol, 2018; 115, 315−28.
8. Tong F, Zhou XM. The Nrf2/HO-1 pathway mediates the antagonist effect of L-arginine on renal ischemia/reperfusion injury in rats. Kidney Blood Press Res, 2017; 42, 519−29.
9. Moncada S, Higgs A. The L-arginine-nitric oxide pathway. N Engl J Med, 1993; 329, 2002−12.
10. O'Donoghue N, Sweeney T, Donagh R, et al. Control of choline oxidation in rat kidney mitochondria. Biochim Biophys Acta, 2009; 1787, 1135−9.

Supplementary Methods

Animals

Forty male Kunming mice, weighing between 27 and 34 g, were purchased from Weitong Lihua Laboratory Animal Technology Co. Ltd. (Beijing, China) and maintained in standard environmental conditions as described in our previous study[1]. All the animal experiments were approved by the Committee on the Ethics of Animal Experiments of the Qiqihar Medical University (Qiqihar, China; Approval number QMU-AECC-2022-136).

Study Design

The test animals were administered RoundUp® (41% isopropyl amine salt, Monsanto, St, Louis, MO, USA) via gavage for 30 days. Thereafter, the mice were randomly assigned to 4 groups (10 mice/group) as described in Supplementary Table S5. The GBH dosage for mice in the high-dose GBH (HG) group was approximately equal to 1/10 the LD50 (oral pathway, 5,600 mg/kg)[2] or the NOAEL of RoundUp® in mice (EPA, 1993). Moreover, it has been confirmed that the 500 mg/kg dose induces sub-chronic to chronic toxicity in mice[3]. The medium and low doses were 1/2 and 1/10 the dosage administered to mice in the HG group, as described in our previous studies[1,4]. After the last herbicide administration, the animals were euthanized via anesthesia using pentobarbital, and their kidneys were collected, weighed, separated, fixed and stored at −80 °C until further analysis.

Measurement of Kidney Function Parameters

Creatinine (CRE), urea nitrogen (BUN), β-N-acetylaminoglucosidase (NAG), and uric acid (UA) were assayed using commercial reagent kits purchased from Jiancheng Bio-Technology Co., Ltd. (Nanjing, China).

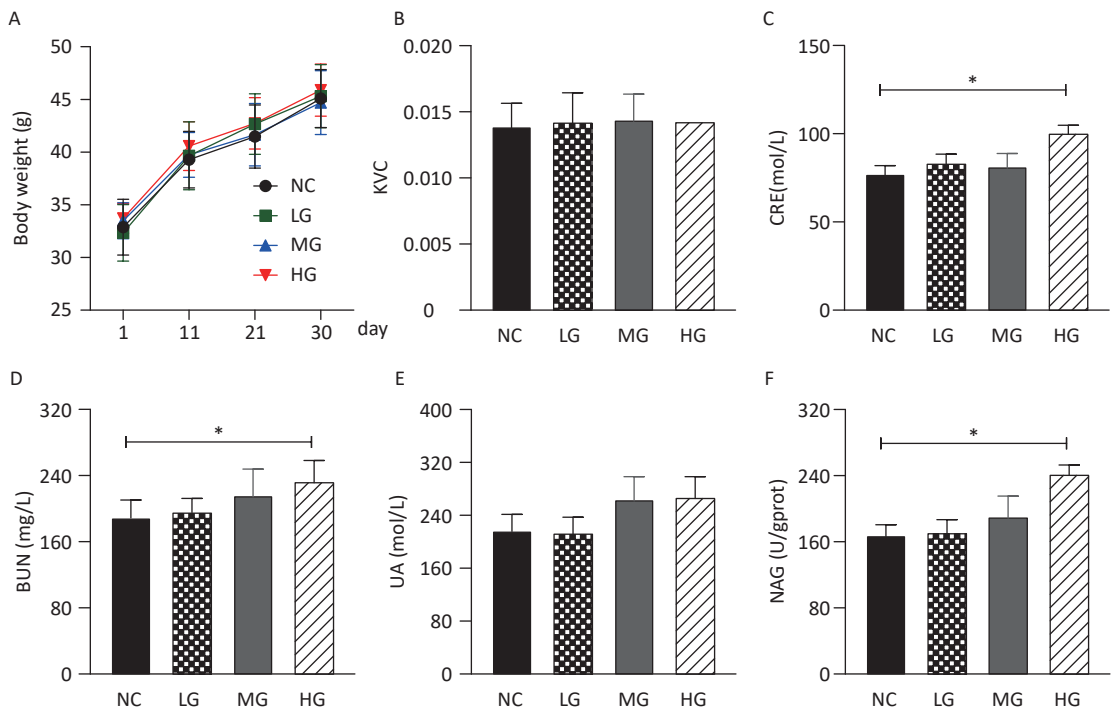

Supplementary Figure S1. The effects of GBH exposure on body weight and kidney function parameters in the serum. A, body weight; B, kidney viscera coefficient; C, CRE; D, BUN; E, UA; F, NAG. Compared with the control group, $^{*}P < 0.05$; $n = 6$. NC, normal control group, 0 mg/kg per day; LG, low dose group, 50 mg/kg per day; MG, middle dose group, 250 mg/kg per day; HG, high dose group, 500 mg/kg per day. Data are presented as means ± SD.

Histological Analysis

Kidney tissue samples were fixed in 4% paraformaldehyde, dehydrated with alcohol, stained with hematoxylin-eosin, and observed *via* light microscopy.

Measurement of Oxidative Stress Indicators of Kidney Samples

OS level in the kidneys of mice from the different groups were assessed using glutathione (GSH), superoxide dismutase (SOD), MDA, catalase (CAT), and total antioxidant capacity (T-AOC) assay kits purchased from Jiancheng Bio-Technology Co., Ltd.

Chromatography, Mass Spectrometry and Data Processing

Six kidney samples from NC and HG groups were randomly selected to perform untargeted metabonomics at Biotree Ltd. (Shanghai, China). Briefly, all samples were pretreated and detected based on a UPLC system (Vanquish, Thermo Fisher Scientific) with a UPLC BEH Amide column (2.1 mm × 100 mm, 1.7 μm) coupled to Q Exactive HFX mass spectrometer (Orbitrap MS, Thermo). The QE HFX mass spectrometer was used to acquire MS/MS spectra based on information-dependent acquisition software (Xcalibur, Thermo), which evaluates the full scan MS spectrum. ProteoWizard was used to convert the raw data to the mzXML format. Further, the data was processed with a new program which was developed using R and based on XCMS, for peak detection, extraction, alignment, and integration. Peaks were pretreated through relative standard deviation de-noising. Then, the missing values were filled up by half of the minimum value. Also, total ion current normalization method was employed in this data analysis. Then an in-house MS2 database (BiotreeDB) was applied in metabolite annotation. The cutoff for annotation was set at 0.3.

SIMCA16.0.2 software package (Sartorius Stedim Data Analytics AB, Umea, Sweden) was used to perform a multivariate analysis of the final dataset. Supervised orthogonal projections to latent structures-discriminate analysis (OPLS-DA) was created to visualize the separation between two groups and identified significantly

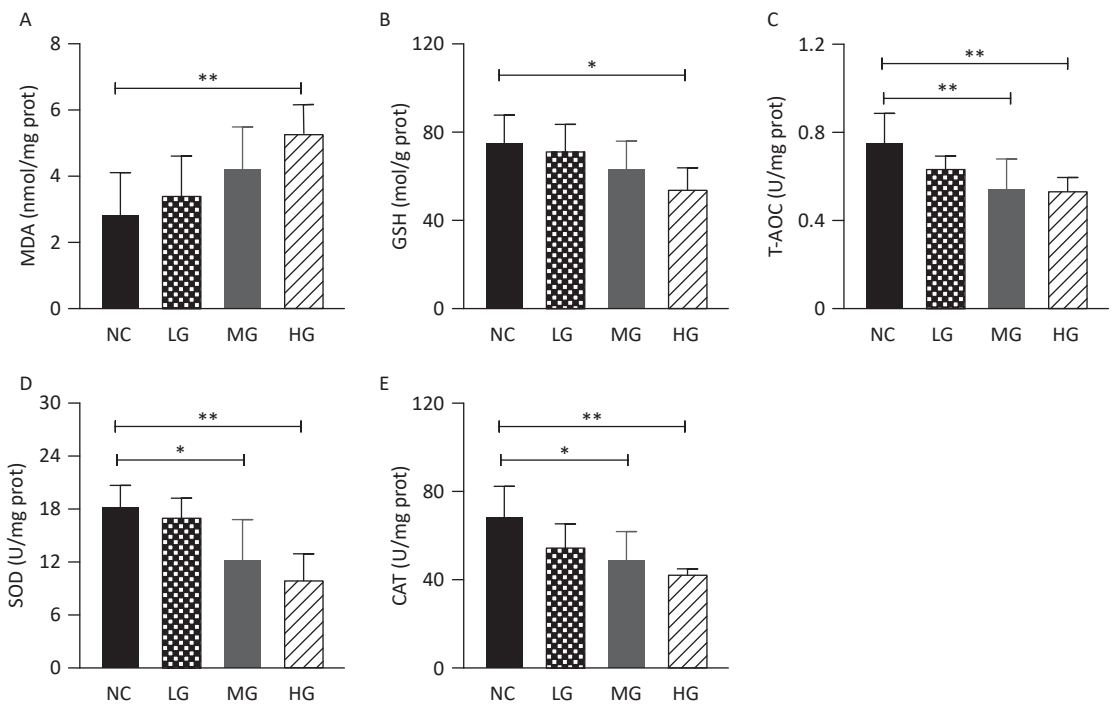

Supplementary Figure S2. The effect of GBH exposure on histopathology in kidneys of male mice. A-H, HE-stain magnification; A B, C and D, 100×; E, F, G and H, 400×. Black arrow: water degeneration; blue arrow: protein deposition in renal tubules. *n* = 6. NC, normal control group, 0 mg/kg per day; LG, low dose group, 50 mg/kg per day; MG, middle dose group, 250 mg/kg per day; HG, and high dose group, 500 mg/kg per day.

changed metabolites (SCMs). Moreover, 200 times permutations were conducted to check the robustness and predictive ability of the OPLS-DA model. The compound with $P < 0.05$ (student t-test) and the value of variable importance in the projection (VIP) > 1 was considered as SCM. All SCMs were annotated to the Kyoto Encyclopedia of Genes and Genomes databases (KEGG, http://www.genome.jp/kegg/) for pathway enrichment analysis.

Statistical Analysis

Group comparisons to identify significant differences were realized via one-way analysis of variance and post-hoc Dunnett's test based using SPSS software version 17.0 (Beijing Stats Data Mining Co. Ltd., Beijing, China). Pearson's correlation analyses were also performed to identify correlations between kidney function indices, SCMs and OS indices. Statistical significance was set at $P < 0.05$.

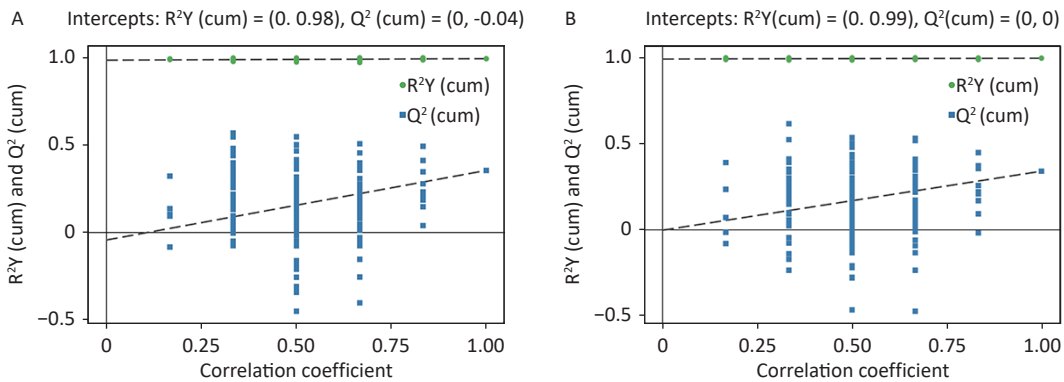

Supplementary Figure S3. Permutation test of OPLS-DA model in the positive and negative ion modes. A, permutation test of OPLS-DA model in the positive ion mode; B, permutation test of OPLS-DA model in the negative ion mode. $n = 6$.

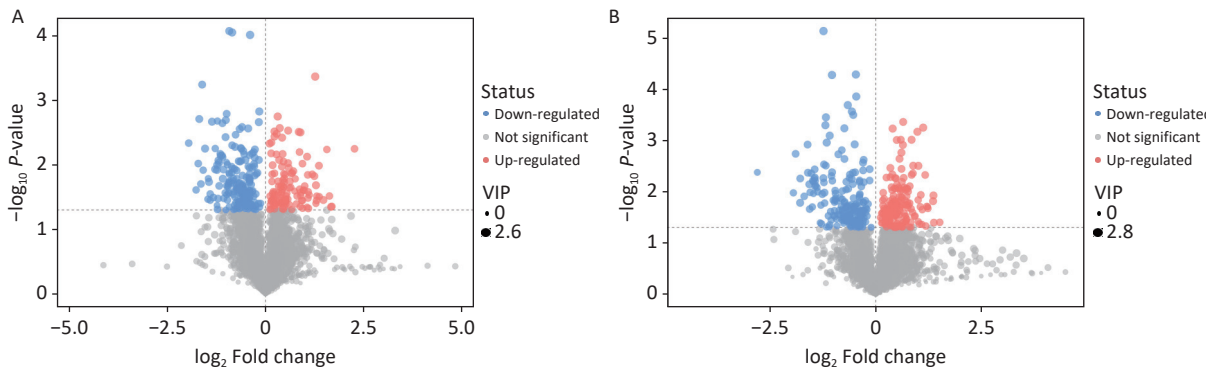

Supplementary Figure S4. Volcano plots in the positive and negative ion modes. A, volcano plot in the positive ion mode; B, volcano plot in the negative ion mode. $n = 6$.

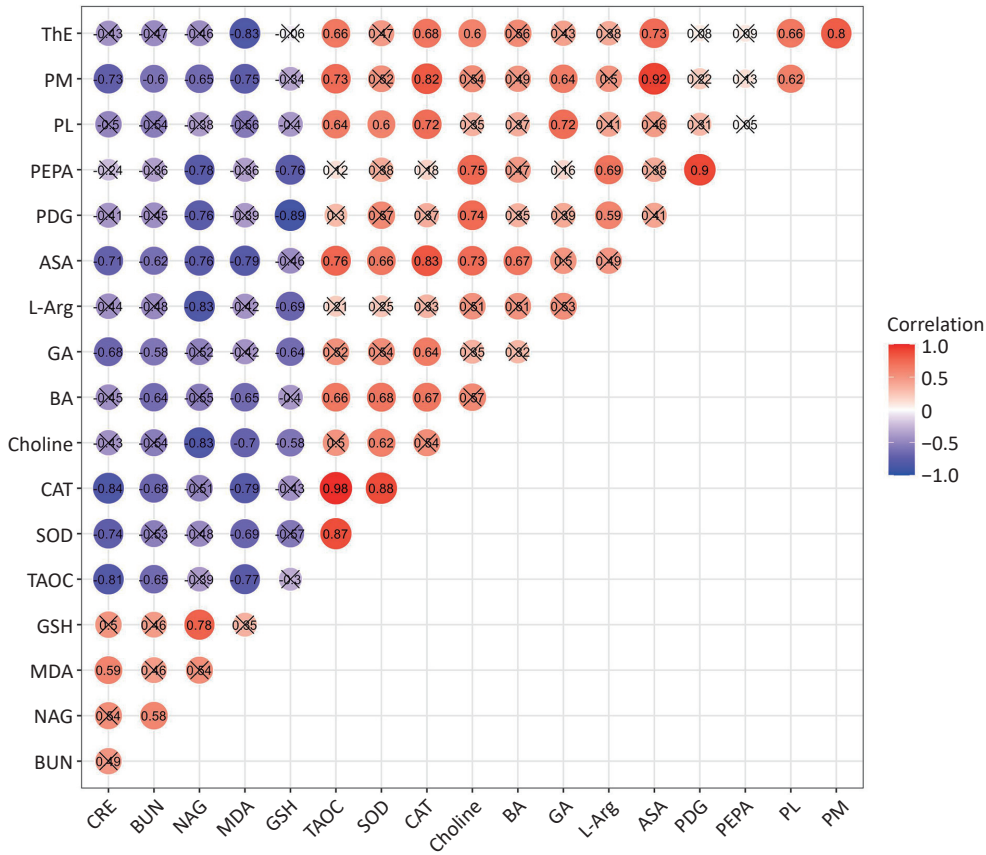

Supplementary Figure S5. Correlation analysis between kidney function indexes and oxidative stress indicators and SCMs. Red indicates that the correlation coefficient greater than 0, and blue indicates that the correlation coefficient lower than 0; the number represents the value of the correlation coefficient; the dot without × indicates that there is statistical difference, the dot with × indicate that there is no statistical difference of correlation. PM, pyridoxamine; PL, pyridoxal; ASA, argininosuccinic acid; GA, D-Glucuronic acid; BA, betaine aldehyde; PDG, 2-phospho-D-glyceric acid; PEPA, phosphoenolpyruvic acid; L-Arg, L-arginine; CRE, creatinine; BUN, urea nitrogen; NAG, β-N-acetylaminoglucosidase; MDA, malondialdehyde; GSH, glutathione; CAT, catalase; T-AOC, total antioxidant capacity; SOD, superoxide dismutase. n = 6.

Supplementary Table S1. SCMs in the positive mode between NC and HG groups (*n* = 6)

Compounds	rt	mz	KEGG ID	VIP	*P*-value	Fold change
Argininosuccinic acid	485.52	291.13	C03406	2.43	0.010	0.43
Choline	299.16	104.11	C00114	2.34	0.002	0.89
Deoxyuridine	180.59	229.08	C00526	2.32	0.003	1.29
Purine	105.16	121.05	C15587	2.02	0.036	0.71
L-Gulose	324.54	203.05	C15923	1.91	0.036	1.92
Histamine	417.27	112.09	C00388	1.90	0.021	0.50
Betaine aldehyde	376.90	102.09	C00576	1.89	0.033	0.74
3-Dehydrosphinganine	85.62	300.29	C02934	1.84	0.034	1.16
Thiamine	386.22	265.11	C00378	1.82	0.047	0.70
Glycitein	43.42	285.08	C14536	1.80	0.035	0.61
N-Acetylhistidine	367.64	198.09	C02997	1.80	0.033	2.11
Queuine	286.50	278.12	C01449	1.77	0.027	0.63
3-Methylguanine	207.89	166.07	C02230	1.77	0.020	0.60
Galactosylhydroxylysine	548.73	325.16	C05547	1.75	0.016	0.75
5-Amino-6-ribitylamino uracil	313.06	277.12	C04732	1.73	0.048	1.35
Pyridoxamine	325.71	169.10	C00534	1.64	0.048	0.59
p-Aminobenzoic acid	41.83	138.05	C00568	1.58	0.048	0.74
Pyridoxal	41.66	168.07	C00250	1.35	0.039	0.59

Supplementary Table S2. SCMs in the negative mode between NC and HG groups (*n* = 6)

Compounds	rt	mz	KEGG ID	VIP	*P*-value	Fold change
Argininosuccinic acid	486.86	289.11	C03406	2.56	0.001	0.45
2-Phospho-D-glyceric acid	477.03	184.98	C00631	2.33	0.006	0.37
Phosphoenolpyruvic acid	491.77	166.97	C00074	2.21	0.037	0.62
Xanthosine	240.10	283.07	C01762	2.15	0.006	0.77
D-Glucuronic acid	403.82	193.03	C00191	1.99	0.020	0.74
Eicosadienoic acid	40.56	307.26	C16525	1.94	0.016	0.77
D-Malic acid	416.64	133.01	C00497	1.93	0.017	0.43
L-Arginine	542.01	173.10	C00062	1.87	0.039	0.77
Deoxyribose 5-phosphate	184.19	213.02	C00673	1.87	0.033	1.18
Terephthalic acid	373.64	165.02	C06337	1.81	0.026	1.10
Beta-D-Galactose	319.55	179.06	C00962	1.78	0.038	2.01
Pentadecanoic acid	42.26	241.22	C16537	1.77	0.027	0.81
3-(3,4-Dihydroxy-5-methoxy)-2-propenoic acid	386.63	209.04	C05619	1.74	0.041	1.10
D-Ornithine	540.85	131.08	C00515	1.15	0.042	0.59

Supplementary Table S3. The information of pathways in the positive mode (NC *vs*. HG) (*n* = 6)

Pathway	Total	Hits	*P*	Impact	Hits Cpd
Vitamin B6 metabolism	9	2	0.005	0.569	Pyridoxal; Pyridoxamine
Glycine, serine and threonine metabolism	31	2	0.051	< 0.001	Choline; Betaine aldehyde
Thiamine metabolism	7	1	0.081	0.400	Thiamine
Riboflavin metabolism	11	1	0.125	< 0.001	5-Amino-6-ribitylamino uracil
Histidine metabolism	15	1	0.166	0.220	Histamine
Sphingolipid metabolism	21	1	0.225	0.083	3-Dehydrosphinganine
Alanine, aspartate and glutamate metabolism	24	1	0.253	0.022	Argininosuccinic acid
Glycerophospholipid metabolism	30	1	0.306	0.023	Choline
Pyrimidine metabolism	41	1	0.395	0.021	Deoxyuridine
Arginine and proline metabolism	44	1	0.417	0.024	Argininosuccinic acid

Supplementary Table S4. The information of pathways in the negative mode (NC *vs.* HG, *n* = 6)

Pathway	Total	Hits	P	Impact	Hits Cpd
Glycolysis or Gluconeogenesis	26	2	0.022	0.201	Phosphoenolpyruvic acid ; 2-Phospho-D-glyceric acid
D-Arginine and D-ornithine metabolism	4	1	0.036	< 0.001	D-Ornithine
Arginine and proline metabolism	44	2	0.059	0.106	Argininosuccinic acid; L-Arginine
Ascorbate and aldarate metabolism	9	1	0.080	0.400	D-Glucuronic acid
Pentose and glucuronate interconversions	16	1	0.138	< 0.001	D-Glucuronic acid
Starch and sucrose metabolism	19	1	0.162	< 0.001	D-Glucuronic acid
Pentose phosphate pathway	19	1	0.162	0.068	Deoxyribose 5-phosphate
Citrate cycle (TCA cycle)	20	1	0.169	< 0.001	Phosphoenolpyruvic acid
Pyruvate metabolism	23	1	0.192	< 0.001	Phosphoenolpyruvic acid
Alanine, aspartate and glutamate metabolism	24	1	0.200	0.022	Argininosuccinic acid
Inositol phosphate metabolism	28	1	0.229	< 0.001	D-Glucuronic acid
Biosynthesis of unsaturated fatty acids	42	1	0.325	< 0.001	Icosadienoic acid
Purine metabolism	68	1	0.474	< 0.001	Xanthosine
Aminoacyl-tRNA biosynthesis	69	1	0.479	< 0.001	L-Arginine

Supplementary Table S5. Glyphosate doses for all treatment groups

Group	Abbreviation	Dose of glyphosate
Control group	NC	0 mg/kg per day
Low-dose GBH group	LG	50 mg/kg per day
Medium-dose GBH group	MG	250 mg/kg per day
High-dose GBH group	HG	500 mg/kg per day

REFERENCES

1. Qi L, Li Y, Dong Y, et al. Integrated metabolomics and transcriptomics reveal glyphosate based-herbicide induced reproductive toxicity through disturbing energy and nucleotide metabolism in mice testes. Environ Toxicol, 2023; 38(8), 1811-1823.
2. FAO/WHO, *Pesticide Residues in Food* 2016, FAO/WHO: Rome, Italy, .
3. Bali YA, Kaikai NE, Ba-M'hamed S, et al. Learning and memory impairments associated to acetylcholinesterase inhibition and oxidative stress following glyphosate based-herbicide exposure in mice. Toxicology, 2019; 415, 18–25.
4. Qi L, Dong YM, Chao H, et al. Glyphosate based-herbicide disrupts energy metabolism and activates inflammatory response through oxidative stress in mice liver. Chemosphere, 2023; 315, 137751.